



Assessment of Physiological Stress and Bark Beetle-Induced Mortality in Fir Trees, Zao Mountains, Japan

Anna Trigubenko ^a, Maximo Larry Lopez Caceres ^a, Hisaya Shimizu ^a, Tatiana A. Shestakova ^{b,c},
Vladislav Bukin ^a, Noboru Kojima ^a

^a Faculty of Agriculture, Yamagata University, Tsuruoka, Japan;

^b Department of Agricultural and Forest Sciences and Engineering, University of Lleida, Lleida,
Spain;

^c Joint Research Unit CTFC–AGROTECNIO–CERCA, Lleida, Spain.

Correspondence to: Anna Trigubenko (annya.tri.99@gmail.com), Maximo Larry Lopez Caceres
(larry@tds1.tr.yamagata-u.ac.jp)

Abstract

In the Northern Hemisphere, bark beetles are responsible for high tree mortality rates in forest ecosystems. In recent decades, forest pest outbreaks have increased in frequency and scale related to climate change. Although, many studies have focused on the effect of pest outbreak on forests, there are few studies focusing on the early physiological stress on trees preceding the infestations. In the treeline of Zao Mountains in northeastern Japan, a double pest infestation of totrix moth (*Epitonina piceae*) and bark beetles (*Polygraphus Proximus*) that caused severe tree mortality in a natural fir forest (*Abies mariesii*), which is the first reported case worldwide of



23 treeline retreat caused by bark beetle infestation. In order to understand forest dynamics prior to
24 the outbreak, tree rings samples were collected from 20 trees in the treeline (dead trees) and 40
25 trees from living trees (healthy and damaged) at lower altitudes. In these samples a
26 dendrochronological and carbon stable isotope analysis ($\Delta^{13}\text{C}$) was performed. Results indicate a
27 declining trend in tree-ring indices (TRI) for dead trees, while living trees showed a strong an
28 annual fluctuation, but did not show any declining trend. Healthy and damaged trees maintained
29 relatively stable $\Delta^{13}\text{C}$ values (14.9‰ - 18.5‰), reflecting stable physiological activity even in the
30 partially defoliated damaged trees. During the years the infestation lasted, there was no response
31 from tree rings $\Delta^{13}\text{C}$ (16.2‰ and 16.4‰) to its surrounding environment in trees prior to their
32 death. The decreasing trend of $\Delta^{13}\text{C}$ values in tree rings prior to pest infestation in dead trees
33 indicate a continuous decline in tree physiological activity caused by a tendency to close the
34 stomata due to environmental stress. In Zao Mountains evidence shows that extreme events in
35 winter lead to severe physical damage in trees, including fallen trees, caused by a combination of
36 heavy snow, strong winds and recently observed high snow density. We speculate that this event
37 gradually weakened trees in the treeline. Another factor that is probably related to this trend is the
38 earlier snowmelt observed in the last two decades, which leads to decreases in soil moisture during
39 spring, when precipitation is the lowest. These findings suggest that $\Delta^{13}\text{C}$ values in tree rings can
40 serve as early warning indicators of stress preceding severe natural disturbance and can contribute
41 to scientific based informing forest management strategies.

42

43 **1 Introduction**

44 Insect outbreaks appear to be increasing in frequency and intensity, a trend probably linked
45 to climate change (Agne et al., 2018; Jactel et al., 2019; Przepiora et al., 2020). Globally, insect-
46 disturbed forests span 85.5 million hectares, representing 3% of the total forested area (2807
47 million hectares) across boreal, temperate, and tropical regions (van Lierop et al., 2015). This
48 alarming trend underscores the need for improved understanding of the drivers and impacts of



49 such disturbances. Bark beetle-induced mass forest mortality has become a large-scale
50 destabilizing factor for forest ecosystems worldwide in recent decades (Cole and Amman, 1980;
51 Pavlov et al., 2020).

52 Among insect species responsible for widespread damage, *Polygraphus proximus*, a non-
53 aggressive phloephagous bark beetle, has garnered significant attention due to its detrimental
54 effect on environmentally disturbed forests. Native to northeastern China, Korea, Japan, and the
55 southern part of the Russian Far East (Nobuchi, 1966; Koizumi, 1977; Kerchev, 2014), this insect
56 has invaded Western Siberia and European Russia, where it has devastated vast areas of fir forests
57 over the past decade (Kononov et al., 2016; Kharuk et al., 2019). In Japan, *Polygraphus proximus*
58 has caused extensive damage to *Abies* species (Tokuda et al., 2008; Takagi et al., 2018, 2021;
59 Chiba et al., 2020), threatening the ecological stability of these forests.

60 As with other bark beetles, once *Polygraphus proximus* populations reach outbreak levels,
61 they are capable of infesting even healthy trees. Such outbreaks, similar to those caused by the
62 mountain pine beetle (*Dendroctonus ponderosae*), have led to the mortality of seemingly healthy
63 trees across millions of hectares. In Zao Mountains, a large-scale bark beetle outbreak between
64 2012 and 2016 resulted in the devastation of pristine *Abies mariesii* forests over hundreds of
65 hectares, especially those close to the treeline. This outbreak has drastically altered the landscape
66 and is expected to have long-term ecological consequences in the region. Bark beetle infestations
67 not only reduce timber production and quality but also disrupt nutrient cycling, carbon uptake, and
68 ecosystem biodiversity, highlighting the far-reaching impacts of these disturbances. Bark beetle-
69 induced tree mortality also reduces the recreational and economic value of forests, affecting human
70 health, tourism, and local livelihoods. The study of the dynamics of forest degradation due to insect
71 outbreaks is of paramount importance, especially under climate change. As the affected area is
72 within a national park, the use of chemicals or other potentially harmful materials is prohibited.
73 Thus, it is necessary to identify early warning signals of physiological stress in trees, which could
74 enable proactive measures to be taken to prevent widespread infestation and mitigate its impact.



75 Forecasting tree mortality remains one of the most uncertain aspects of dynamic vegetation models
76 (Bugmann et al., 2019), especially when multiple disturbance factors interact. Identifying early
77 reliable indicators of physiological stress that are informative of, for example, the carbon-water
78 balance of trees is critical for improving predictive capabilities and forest management strategies.

79 Tree rings, which serve as natural archives, capture annual-resolution information of radial
80 growth and the environmental conditions at the time of tree ring formation. Among the most
81 important tools used in conjunction with dendrochronology, stable carbon isotope analysis of
82 individual rings stands as a powerful method for evaluating environmental influences on tree
83 physiology. Declining annual ring width, coupled with increasing carbon isotope ratios ($\delta^{13}\text{C}$), has
84 been correlated with reduced photosynthetic activity and stomatal closure, preceding tree mortality
85 by several years (Gessler et al., 2002; Cailleret et al., 2017). These patterns underscore the value
86 of tree-ring analysis and stable isotope studies in unraveling the complex interplay of climatic and
87 biotic factors influencing forest dynamics. Long-term decreases in annual ring width coupled with
88 increasing trends in $\delta^{13}\text{C}$ can be used as early warning signals of physiological stress and recovery
89 of trees when subjected to severe disturbances (Lopez et al., 2018). Advanced dendrochronological
90 and isotopic approaches are key to understanding the interactions between physiological stress,
91 climatic variables, and bark beetle activity. By combining detailed growth and isotopic data with
92 regional climate records, predictive models can be developed to identify high-risk areas and inform
93 adaptive forest management practices (McCarroll and Loader, 2004; Bugmann et al., 2019).

94 The host species in this study, *Abies mariesii*, commonly known locally as Ooshirabiso, is
95 an evergreen tree native to subalpine regions of Japan, which is usually found at elevations ranging
96 from 1300 to 2900 meters. Fir forest thrives in cold temperate rainforests characterized by high
97 rainfall and heavy snow (Tanaka and Matsui, 2007). These trees, which typically grow to heights
98 of 10 to 30 meters, play a critical role in maintaining ecosystem stability in Japan's mountainous
99 regions. However, the sudden loss of *Abies mariesii* due to bark beetle outbreaks has led to the
100 near-total collapse of forest ecosystems in the treeline (Chiba et al., 2017).



101 In this study, we hypothesize that the combined effects of environmental factors in Zao
102 Mountains in recent decades have affected stomatal conductance and intercellular CO₂
103 concentrations, leading to changes in wood isotopic signatures. Therefore, the specific objectives
104 of this study are:

- 105 1. To determine the tree growth pattern of fir trees three decades prior to pest infestation;
- 106 2. To compare the carbon isotope signatures (carbon isotope discrimination, $\Delta^{13}\text{C}$) of
107 healthy, damaged and dead trees (before death in 2016) and evaluate their
108 environmental control for each of the health categories from 1993 to 2022.

109

110 **2 Methodology**

111 **2.1 Study site**

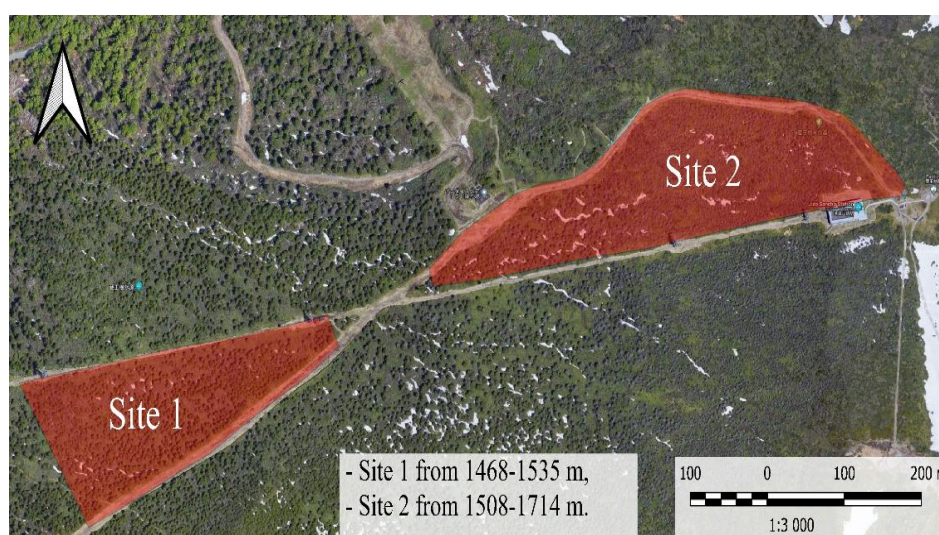
112 Zao Mountains are located in an active volcanic range on Honshu Island, in northeastern
113 Japan on Honshu Island (38.14°N, 140.44°E), representing a region of ecological significance and
114 biodiversity. Spanning 11 hectares within Yamagata Prefecture, the study area is situated at the
115 border of Yamagata and Miyagi prefectures. The forest composition includes both pure stands of
116 Maries fir (*Abies mariesii*) at higher altitudes and broadleaf mixed forests interspersed with a few
117 deciduous and coniferous species such as *Fagus crenata*, *Acer tschonoskii*, and *Sorbus commixta*
118 in lower areas. The understory across the altitudinal gradient is dominated by Sasa grass, which
119 stabilizes soil and enhances nutrient cycling (Nguyen et al., 2021; Tran et al., 2024; Hu et al.,
120 2022).

121 The altitudinal gradient significantly influences forest structure and dynamics. At
122 elevations between 1468 m and 1535 m, tree density averages to 400 trees per hectare, with a
123 marked decline in tree size, height, and canopy area as altitude increases. The dominance of *Abies*
124 *mariesii*, which covers 87% of the forested area - is juxtaposed with patches of mixed coniferous



125 and deciduous vegetation. At higher elevations between 1508 m and 1714 m, close to the treeline,
126 over 92% of fir trees have succumbed to bark beetle (*Polygraphus Proximus*) infestation, resulting
127 in dramatic shifts in forest composition and structure (Fig. 1) (Saito and Chiba, 2017).

128



129

130 **Figure 1.** Study site located in Zao Mountains.

131

132 The ecological setting of Zao Mountains is further complicated by its status as an active
133 volcanic region. Frequent seismic activity, volcanic emissions, and extreme weather events such
134 as typhoons interact with biotic stressors, to shape forest health and resilience (Takagi et al., 2021).
135 These interactions create a dynamic environmental mosaic, making management of those forests
136 a challenging task. The forests of Zao Mountains also hold significant conservation value, serving
137 as carbon sinks and providing critical ecosystem services such as water regulation and biodiversity
138 maintenance. By synthesizing field observations, dendrochronological data, stable isotope records
139 and precise remote sensing information, this study uses an integrative approach which is critical
140 for developing predictive models and site-specific management strategies to mitigate future
141 impacts on subalpine forests in Japan.



142 **2.2 Tree core sampling and preparation**

143 Tree cores were collected in the summer of 2022. Two cores per tree were taken at breast
144 height (1.3 m) from healthy, damaged, and dead individuals using a 5 mm increment borer (Haglöf,
145 Sweden). One core was used for tree-ring dating, while the other was left intact for isotopic
146 analysis. A total of 120 cores were collected, comprising 40 from healthy trees, 40 from damaged
147 trees, and 40 from dead trees. This sampling strategy was designed to disentangle differences in
148 growth and physiological responses between forest health conditions.

149 The preparation of tree-ring samples began with oven drying of the cores at 60°C for 48
150 hours. They were then glued into wooden holders. Hot glue was applied to hold the samples in
151 place, ensuring stability during the subsequent processing steps. A polishing machine was then
152 used to plane and smooth the top surface of the samples, removing irregularities and revealing the
153 tree ring structure. This step improved the visibility of the annual rings for further analysis
154 (Schweingruber, 1988; Stokes and Smiley, 1996).

155 **2.3 Tree-ring analysis**

156 High-resolution images (1000 dpi) of the polished cores were taken using specialized
157 imaging systems. These images were used as the input for the WINDENDRO software (Regent
158 Instruments Inc, Canada). Tree rings were visually cross-dated and measured to an accuracy of
159 0.01 mm. COFECHA was then used to validate the cross-dating of individual cores (Grissino-
160 Mayer, 2001; Holmes, 1983). The software calculates the width of each annual ring, providing
161 precise measurements essential for dendrochronological research.

162 COFECHA was used to validate the master chronology by cross-dating and detecting
163 anomalies in tree-ring data, ensuring reliable $\delta^{13}\text{C}$ analysis (Grissino-Mayer, 2001; Holmes, 1983).
164 Samples with high correlation with the Master chronology were selected for isotopic studies.
165 ARSTAN standardized ring-width data, correcting growth anomalies linked to extreme climatic



166 events, enhancing the accuracy of environmental signal extraction (Cook & Krusic, 2005; Briffa
167 & Melvin, 2011).

168 **2.4 Stable isotope analysis**

169 Four cores that best correlated with the master chronology for each health status were
170 selected for isotopic analysis. Tree rings were manually separated using a fine scalpel under
171 magnification to ensure precise isolation of individual annual layers without cross-contamination.
172 Each ring was then finely cut into small pieces. Small pieces were ultrasonically cleaned in
173 distilled water to remove contaminants while preserving the cellulose structure. Rings
174 corresponding to the same year and health status were pooled into a single sample before analysis
175 (Leavitt 2008), except for every five years when rings were analyzed independently to estimate
176 the between-tree variability in carbon isotopes (Loader et al., 2013). Individual tree rings were
177 preserved for the years 1996, 2001, ..., 2016 for dead trees and for the years 1997, 2002, ..., 2022
178 for living trees. The resulting samples were homogenized using a ball mill. Approximately 0.6-0.8
179 mg of the dry material was weighed using a microbalance, packed in tin capsules, and analyzed
180 by isotope ratio mass spectrometry. Isotope ratios were expressed as per mil deviations using the
181 δ notation relative to Vienna Pee Dee Belemnite (VPDB). The accuracy of the analyses (SD of
182 standards) was 0.06‰.

183 To account for changes in $\delta^{13}\text{C}$ of atmospheric CO_2 ($\delta^{13}\text{C}_{\text{air}}$), we calculated carbon isotope
184 discrimination ($\Delta^{13}\text{C}$) from $\delta^{13}\text{C}_{\text{air}}$ and tree-ring $\delta^{13}\text{C}$ ($\delta^{13}\text{C}_{\text{wood}}$) following (Eq 1) (Farquhar et al.,
185 1982; Farquhar and Richards, 1984):

$$186 \quad \Delta^{13}\text{C} = \frac{(\delta^{13}\text{C}_{\text{air}} - \delta^{13}\text{C}_{\text{wood}})}{1 + \delta^{13}\text{C}_{\text{wood}}/1000} (\text{‰}) \quad (1)$$

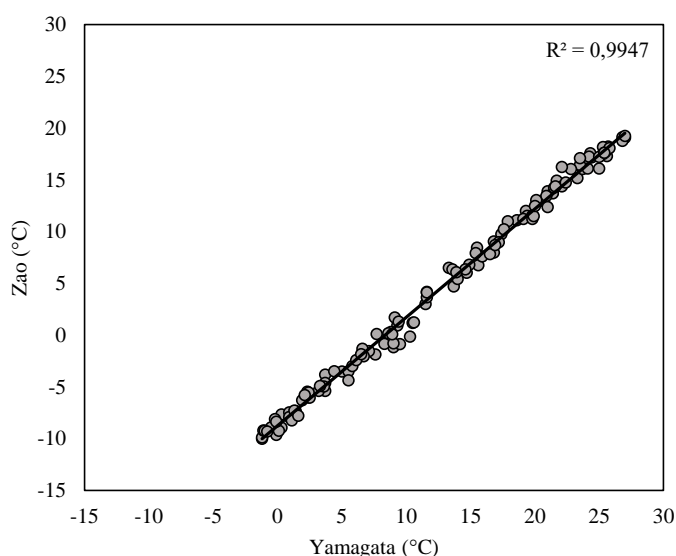
187 **2.5 Meteorological data**

188 Meteorological data for this study were collected at facilities of the Zao ropeway in Jizo
189 Mountain, located at 1676 m.a.s.l. The meteorological data include wind speed and direction, snow



190 depth, and temperature. Freeze-thaw cycles, high diurnal variability in air temperature, high
191 precipitation and strong western winds are the normal conditions in this region. Since
192 meteorological data from the Zao station is only available from 2012, a comparative analysis was
193 conducted using data from the nearby meteorological station at Yamagata city to extend the
194 temporal range. A comparative analysis over the common period (2012-2022) showed high
195 correlation between the monthly mean temperature of the two stations ($r=0.99$) (Fig. 2).
196 Consequently, the temperature data (mean, minimum, maximum) from the Yamagata station was
197 used as the primary source of climate information.

198



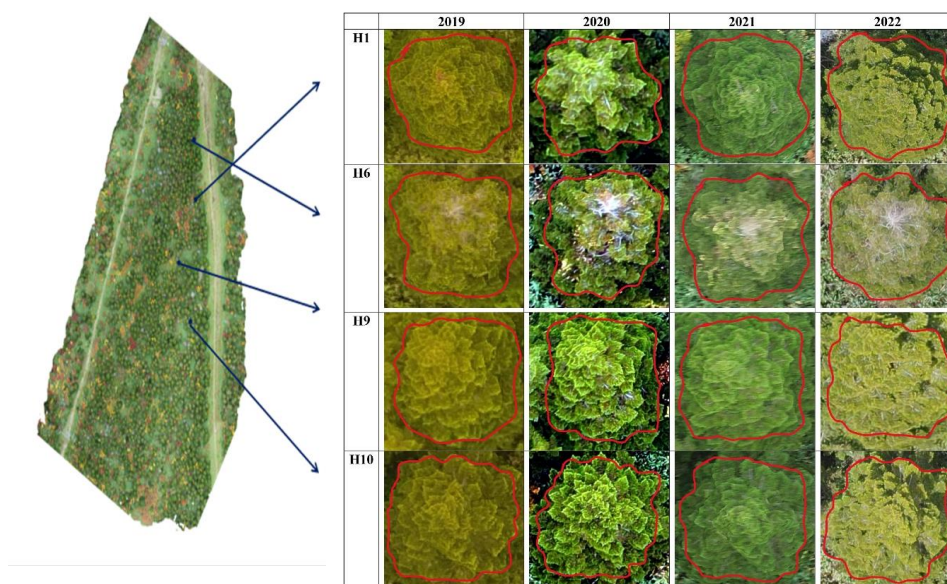
199

200 **Figure 2.** Correlation between monthly mean temperature records from the Zao ropeway facilities and
201 Yamagata meteorological station over the period 2012-2022.

202

203 2.6 Unmanned Aerial Vehicles

211



214

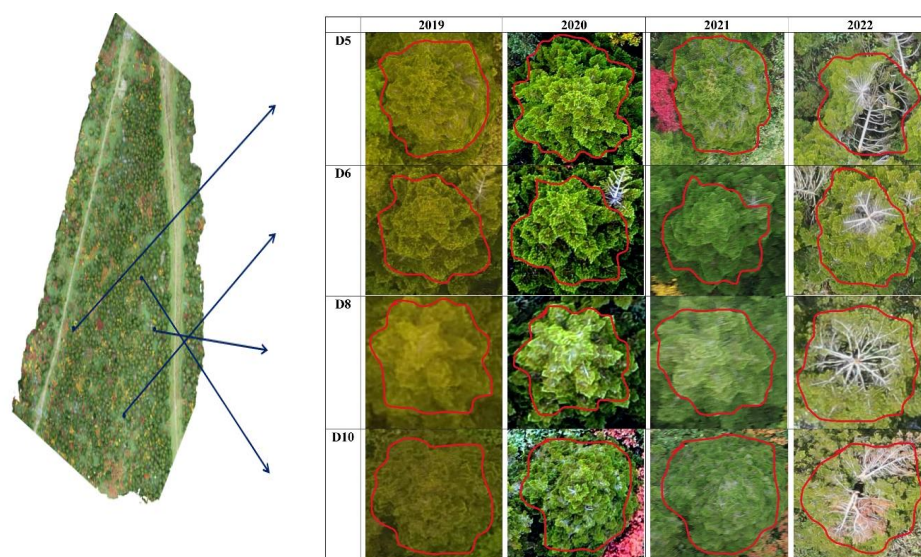


Figure 4. Chronological crown condition of some representative damaged (D) trees in orthomosaics for period 2019-2022.

3 Results

3.1 Tree-ring index

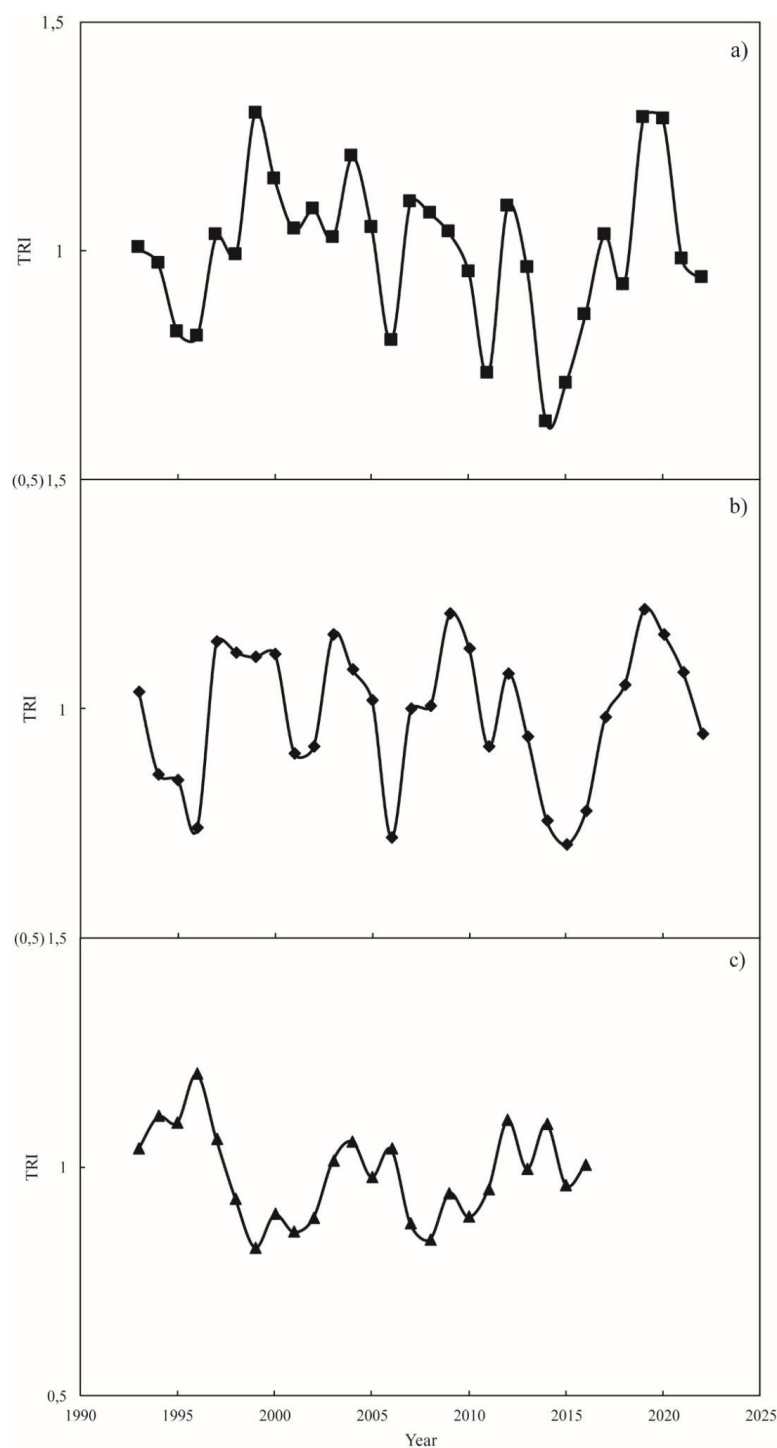
The analysis of tree-ring indices (TRI) for healthy, damage, from 1993 to 2022 and for dead trees 1993 to 2016 provides significant insights into tree growth dynamics and responses to its environmental surroundings. The study period captured critical climatic and ecological variations influencing forest health and resilience prior to pest infestation (Fig. 5).

Healthy and damaged trees were located at the same altitude and belonged to the same forest area. Tree-ring growth represented by indexed tree-ring chronologies (TRI) for these two health categories did not always have the same annual pattern, but most narrow and wide rings were observed in the same years. The range of TRI values was similar for healthy trees (0.623-1.300) and damaged trees (0.703-1.215), despite a difference in canopy defoliation observed between the four trees classified as damaged and those with no defoliation, classified as healthy.



230 In the case of dead trees, they were located at higher altitudes with a different climate than that of
231 healthy and damaged trees, hence the different values observed in TRI during the period prior to
232 their death. For dead trees, the last year was determined based on the year when most of trees died
233 among the 20 samples. TRI of healthy and damaged trees did not show a clear trend in the last 30
234 years. In contrast, dead trees showed a decreasing trend, especially from the year 1998, where a
235 clear shift to lower values was observed. Furthermore, the annual variability of tree-ring growth
236 was much lower over the past two decades, compared to the higher variability observed in the
237 1990s, or the higher variability observed for the TRI values of healthy and damaged trees.

238



239

240 **Figure 5.** Trends in Tree Ring Index (TRI) from 1993-2022 for a) healthy, b) damaged, and c) dead trees.



241 **3.2 Carbon isotope discrimination ($\Delta^{13}\text{C}$)**

242 $\Delta^{13}\text{C}$ for the healthy trees remained relatively stable over the period 1993-2022 with values
243 ranging from 14.9‰ to 18.5‰ with no clear trend for the last 30 years (Fig. 6a). In comparison,
244 $\Delta^{13}\text{C}$ values for damaged trees showed a smaller range from 16.5‰ to 17.9‰ (Fig. 6 b). Healthy
245 trees as well as damaged trees showed an increasing trend, especially from the beginning of the
246 year 2000s, however the annual variability of $\Delta^{13}\text{C}$ values is smaller in damaged trees compared
247 to the healthy ones. The composite oscillation with periodic individual sampling approach showed
248 that the years chosen for multiple carbon isotope measurements represented well, the composite
249 values as shown by the similar values found in the years when 4 individual samples were measured.
250 There are some outliers as in 2018 in the healthy tree $\Delta^{13}\text{C}$ values but they show a steady trend.

251 In general, healthy and damaged trees did not show negative trends for the last 30 years,
252 while $\Delta^{13}\text{C}$ values of dead trees for the period 1993-2016, showed a clear decreasing trend already
253 from the start of the measuring period. The values oscillated within the range of 15.8‰ and 17.4‰
254 (Fig. 6c), with a clear annual variability for the period 1993- 2012, however, for the years 2012-
255 2016, there is no response of $\Delta^{13}\text{C}$ to annual environmental variability, as the values remain the
256 same for these years, which coincides with the pest infestation reported in this region.

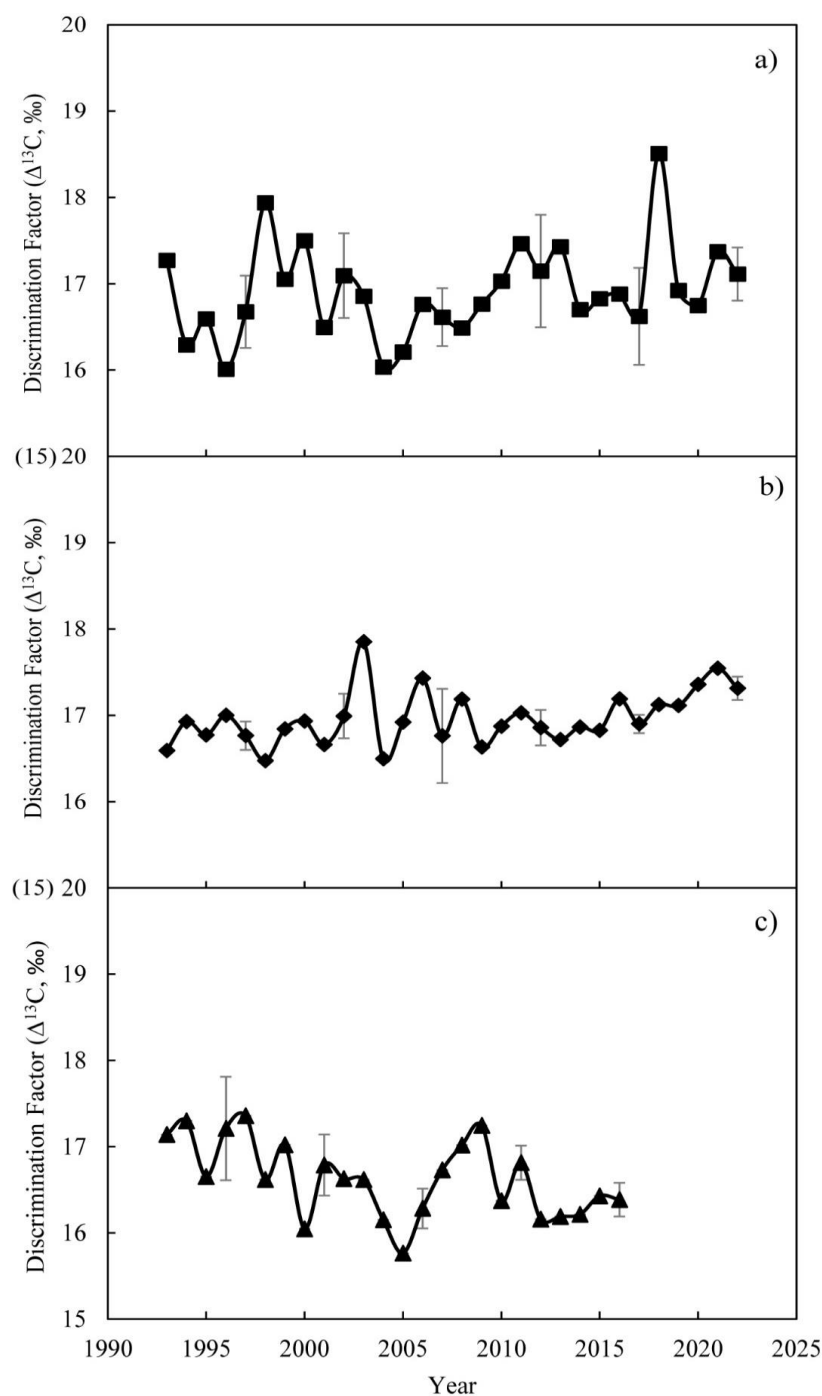
257

258

259

260

261





263 **Figure 6.** Carbon isotope discrimination ($\Delta^{13}\text{C}$) trends from 1993-2022 for a) healthy trees b) damaged
264 trees and c) dead trees. Error bars indicate the standard error of selected years for individually analyzed
265 trees.

266

267 **3.3 Environmental conditions**

268 Based on the strong correlation between air temperatures in Jizo Mountain and Yamagata
269 City, the annual average, minimum and maximum air temperatures from 1993 to 2022 data of
270 Yamagata city were examined (Fig. 7, a). Over the years, there is a clear upward trend in both
271 minimum and maximum temperatures, indicating a gradual warming. It appears that in the last 5
272 years, starting in 2018 to 2022, annual temperature remained the same with no clear annual
273 variability. Summer (June-August) vapor pressure deficit (VPD) data ranged from 0.5 to 0.9 from
274 1993 to 2022 (Fig. 7b). A peak was observed for the years 2010-2013, followed by a decline and
275 low annual variability in the last 5 years, with an average value for these years of 0.7 kPa.

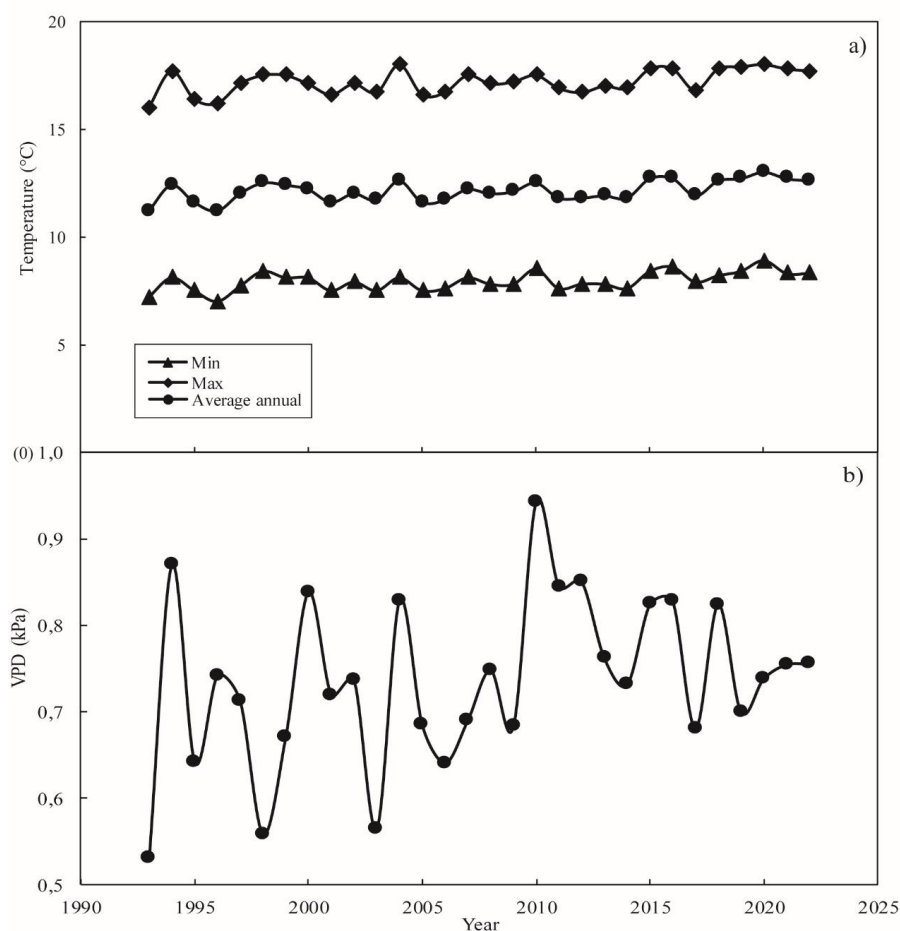


Figure 7. a) Average annual air temperature Trends in Yamagata (1993-2022); b) Summer (June-August) vapor pressure deficit (VPD) in Zao Mountain (1993-2022).

The analysis of snow depth data for Zao Mountain from 2012 to 2022 reveals significant seasonal and inter-annual variability (Fig. 8). The annual average snow depth ranged from 100 cm to 260 cm. The maximum value was observed in 2014 (260 cm) and the minimum during this period was reported in 2020 (100 cm). A peak after bark beetle infestation was recorded in 2018 (230 cm). From 2012 to 2020, a slight decreasing was observed, however, in the last three years



(2020-2022), a slight increase in snow depth has been observed, reflecting the unpredictability of winter precipitation and accumulation patterns.

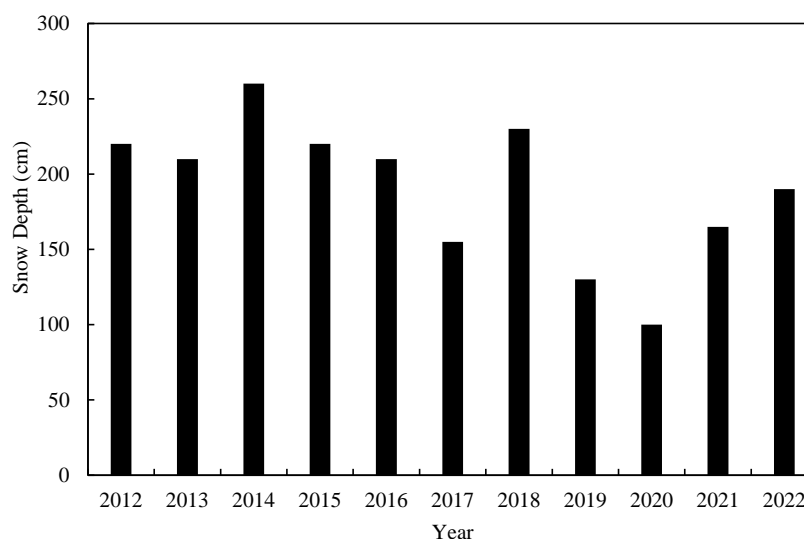


Figure 8. Annual Average Snow Depth in Zao Mountain (2012-2022).

Westerly winds dominated throughout the year, with particularly high wind activity during the winter months (December to February). During this period, wind speeds frequently ranged from 0 to 20 m/s, exceeding those recorded during the summer months. The west (W) direction was dominant in the area, accounting for 63% of the total wind occurrences (Fig. 9). The southwest (SW) direction is the second most frequent, contributing 12%, followed by northwest (NW) with 10%. Together, these three directions account for 85% of the total wind occurrences. Other directions, such as south (S) with 7% and southeast (SE) with 3%, show limited influence, while directions like north (N), east (E) and northeast (NE) collectively made up only 5% of the wind direction patterns.

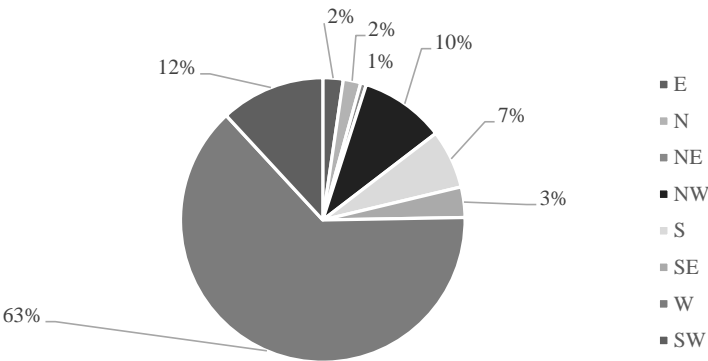


Figure 9. Wind direction distribution (2012-2022) in the Zao Mountains.

4 Discussion

The results of this study provide crucial insights into the difference in tree growth and physiological responses of *Abies mariesii* to environmental conditions prior to bark beetle infestations in the Zao Mountains. By analyzing annual ring width and stable isotope discrimination over the past three decades (period 1993-2016 for dead trees and 1993- for healthy and damaged trees), important signs of physiological stress preceding mortality were identified.

4.1 Tree ring growth and carbon isotope discrimination

Bark beetle infestations can lead to a decrease in tree-ring $\Delta^{13}\text{C}$ as plant carbon assimilation process is negatively affected. Results show that decreasing annual ring width coupled with decreasing carbon isotope discrimination ($\Delta^{13}\text{C}$) values can serve as early-warning signals of the long-term forest weakening that can lead to tree mortality when pest outbreaks occur. The decline of $\Delta^{13}\text{C}$ values in trees located in the treeline aligns with previous studies indicating that impaired stomatal conductance and reduced carbon assimilation reflect the effect of severe disturbances on trees (Lopez et al., 2018).



317 The trends in healthy tree TRI indicate that trees maintained relatively stable growth
318 patterns, while damaged trees exhibited smaller annual fluctuation in recent years, mainly caused
319 by their partial defoliation over the years. The difference between healthy and damaged TRI were
320 small, including higher and lower values during years of higher environmental variability. In
321 contrast, dead trees displayed a gradual decline in TRI values since the early 1990s, emphasizing
322 the cumulative effects of long-term stress which likely led to tree mortality. It is worth noticing
323 that healthy and damaged trees are located at a lower altitude compared to the dead trees growing
324 in the treeline, where trees are exposed to more extreme climate condition. As a result of the bark
325 beetle infestation the treeline in Zao Mountains has receded several hundred meters. Thus, the Zao
326 mountain this is a rare case of treeline recession as described in a meta-analysis by Harsch et al.
327 (2009), that reported that only 1% of all the treelines worldwide had receded vs 52% that had
328 advanced upwards.

329 The average age of trees in the two sites varies from 40-90 years old. Younger trees showed
330 higher ring growth related to higher photosynthesis rates (Ryan and Yoder, 1997) and higher cell
331 production (Rossi et al., 2008). They also use more topsoil water because of their widespread root
332 in the top soil (Børja et al., 2008), while old trees rely more heavily on the use of carbon reserves
333 of previous years, which can have higher $\delta^{13}\text{C}$ values (McCarroll et al., 2017; Timofeeva et al.,
334 2017), resulting in higher tree-ring $\delta^{13}\text{C}$ in old trees. Thus, lower soil moisture from snowmelt
335 could cause a major effect on younger trees, since older trees have deeper roots or can use more
336 reserves in Zao Mountains. However, the long-term stress observed in trees based on the
337 decreasing TRI and ($\Delta^{13}\text{C}$), suggests that the double infestation of *Epitonia piceae* and bark beetles
338 affected equally young and old trees, since tree mortality in this area reached 92%. When trees are
339 attacked by bark beetles, they experience physiological stress, which may affect their carbon
340 assimilation and allocation patterns. The $\delta^{13}\text{C}$ values in tree rings can reflect these changes.
341 However, the specific response of $\delta^{13}\text{C}$ to bark beetle attacks can vary depending on several



342 factors, including the severity of the attack, tree species, and local environmental conditions
343 (Ulrich et al., 2022; Kolb et al., 2019), as we have seen in our study.

344 Our results showed that the bark beetle attack reported in 2012 did not translate in a sharp
345 decrease of $\Delta^{13}\text{C}$ as it has been observed for severe disturbance (Lopez et al., 2018). Instead, a
346 small gradual decrease was observed but it was followed by lack of variation of TRI as well as
347 $\Delta^{13}\text{C}$, representing a loss of sensitivity of trees to their surrounding environment in the last 5 years
348 before death. The effect of *Epitonia piceae* attacks by itself does not necessarily lead to tree
349 mortality as it has been shown by Dulamsuren et al (2010) in larch trees after a severe gypsy moth
350 attack. However, the subsequent attack of bark beetle led to extended tree mortality.

351 Stress, such as the infestation of bark beetle in fir trees, can lead to partial closure of
352 stomata, reducing carbon dioxide uptake during photosynthesis. This can result in a decrease in
353 $\delta^{13}\text{C}$ values, as the plant discriminates less against ^{13}C under conditions of ^{12}C scarcity. Damaged
354 trees remained in the same condition for several years, but it is not clear if in the long term they
355 will recover to their original condition or if they will finally succumb to the infestation as it has
356 been already observed in trees in Zao Mountains.

357 The observed patterns confirm that dead trees experienced significant carbon assimilation
358 reduction before their demise, while healthy trees maintained stable physiological function.
359 Damaged trees showed some fluctuations in $\Delta^{13}\text{C}$ values, suggesting ongoing stress but not yet at
360 levels critical to mortality.

361 One of the reasons why trees in the treeline were attacked by bark beetles and subsequently
362 died was most probably the result of weakening by environmental factors. Other factor such as
363 root diseases, and competition for limited resources can increase stress among trees, could have
364 had an additional effect on increasing tree vulnerability. Trees at lower altitudes are taller and their
365 crowns are larger than in the treeline. Taller trees with more water availability, light, and nutrients
366 are more effective in repelling bark beetle attacks. Smaller vegetation, is the reflection of harsher



367 environmental conditions such as light, soil moisture, wind and snowfall. Milder environmental
368 conditions at lower altitudes provide trees with more suitable conditions to cope with pests or be
369 less susceptible to other disturbances. Rising temperatures and increasingly earlier snowmelt
370 periods can increase droughts especially during the spring period weakening tree defenses and
371 making them more susceptible to bark beetle attacks, although altitude played an important role in
372 the response of fir trees to bark beetle outbreaks as the same devastating effect was not observed
373 in lower altitudes.

374 **4.2 Role of Climatic Factors in Tree Vulnerability**

375 Due to the significant difference in elevation between the two sites, trees in the treeline
376 were exposed to more severe climate conditions, particularly strong wind and heavy snow in
377 winter. Meteorological analysis revealed that air temperatures have been increasing in recent
378 decades, which is leading to early snowmelt, depriving trees of soil moisture in spring. Tree
379 mortality stopped at a defined altitude delineating a clear line in the field by the year 2016, which
380 suggested the importance of elevation as a controlling factor but most importantly, that line appears
381 to represent the change in climate at the bottom of the treeline, at lower altitudes. One more factor,
382 that needs to be taken into account is the snow density, which in given years can cause an extra
383 physical stress on trees if combined with snow depth and usual strong winds increasing the
384 vulnerability of forests observed in the last decade. High wind speeds can increase the risk of
385 windthrow, where trees are uprooted or broken due to the combination of wind force and factors
386 such as soil conditions and root structure (Schindler et al., 2011). As it was observed in the winter
387 of 2021-2022, a large number of healthy trees fell down, usually broken at a height of 3 to 4 meters,
388 leaving fallen trees all over the forest in Site 1. These fallen trees, as it has been reported, can
389 intensify bark beetle reproduction in the disturbed forest (Louis et al., 2014, 2016), and could be
390 the trigger of further forest decline in Site 1 as it probably happened in Site 2. The recent increase
391 in VPD values, related to increases in air temperature, particularly in summer, may indicate further
392 drier air conditions. However, these values have been stable from the year 2011, which is also in



393 agreement with the stability of air temperature during this period. These trends suggest a potential
394 mitigation of extreme climatic conditions in Yamagata, at least for the last years. Despite the
395 physical damage that can be related to heavy snowfall, high snowfall accumulation can insulate
396 soil and tree roots, reducing freeze damage. The high variability of annual average snow depth
397 highlights the influence of larger-scale climatic factors, such as El Niño and La Niña, which can
398 impact snowfall intensity and duration (McClung, 2013).

399

400 **5 Conclusion**

401 This study showed that fir trees that died in the treeline of Zao Mountains as result of severe
402 bark beetle infestation, were in a continuous declining condition as the TRI and $\Delta^{13}\text{C}$ revealed.
403 From the beginning to end of the infestation (2012-2016), especially $\Delta^{13}\text{C}$ lost its sensitivity to
404 environmental factors, as its values remained stable during this period. In comparison, $\Delta^{13}\text{C}$ of
405 healthy and damaged trees, showed an increasing trend, representing better growth conditions and
406 a strong sensitivity to their surrounding environment. The results of this study suggest that carbon
407 stable isotopes can be used as an early warning system to evaluate the condition of vulnerable
408 forests such as those in the treeline. It also shows the first case reported worldwide of treeline
409 recession caused by bark beetle infestation under climate change.

410

411 **Data availability**

412 Data sharing is not applicable to this article.

413 **Sample availability**

414 Sample sharing is not applicable to this article.

415 **Author contribution**



416 A. Trigubenko: conceptualization, methodology, formal analysis, data curation, writing - original
417 draft preparation, visualization, laboratory analysis (stable isotope and dendrochronological
418 analysis), sample preparation, data interpretation.

419 M.L.L. Caceres: conceptualization, methodology, supervision, review and editing, project
420 administration, manuscript revision, critical input on research design, data validation.

421 H. Shimizu: meteorological data analysis, data curation, climate data integration, analysis of
422 environmental variables.

423 T.A. Shestakova: supervision, methodology, writing - review and editing, data validation, critical
424 review of manuscript, conceptual input, ethical and regulatory compliance.

425 V. Bukin: fieldwork coordination, sample collection, UAV data collection and analysis, map
426 creation, visualization, writing - review and editing, field data validation.

427 N. Kojima: laboratory assistance, sample preparation, technical support for stable isotope analysis,
428 data validation, writing - review and editing.

429 **Competing interests**

430 The authors declare that they have no conflict of interest.

431 **Acknowledgements**

432 We gratefully acknowledge the support provided by the members of the Smart Forest Laboratory
433 (Yamagata University) and to the laboratory of Prof. Matteo Garbarino from DISAFA department
434 (University of Torino) for data collection, sample preparation, and laboratory analysis (stable
435 isotope and dendrochronological analysis). Their contributions were crucial to the success of this
436 research.

437 **References**



- 438 Agne, M.C., Beedlow, P.A., Shaw, D.C., Woodruff, D.R., E Lee, H., Cline, S.P., Comeleo,
439 R.L.: Interactions of predominant insects and diseases with climate change in Douglas-fir forests
440 of western Oregon and Washington, U.S.A, For Ecol Manage, 1, 409:317-332,
441 <https://doi.org/10.1016/j.foreco.2017.11.004>, 2018
- 442 Børja, I., De Wit, H. A., Steffenrem, A., Majdi, H.: Stand age and fine root biomass,
443 distribution and morphology in a Norway spruce chrono sequence in Southeast Norway, Tree
444 Physiology, 28 (5), 773-784, <https://doi.org/10.1093/treephys/28.5.773>, 2008
- 445 Briffa, K.R., Melvin, T.M.: A closer look at Regional Curve Standardization of tree-ring
446 records: justification of the need, a warning of some pitfalls, and suggested improvements in its
447 application, In: Hughes, M.K., Diaz, H.F., Swetnam, T.W. (Eds.), Dendroclimatology: Progress
448 and Prospects, Springer Verlag, Dordrecht, 113-145, [https://doi.org/10.1007/978-1-4020-5725-](https://doi.org/10.1007/978-1-4020-5725-0_5)
449 [0_5](https://doi.org/10.1007/978-1-4020-5725-0_5), 2011
- 450 Bugmann, H., Seidl, R., Hartig, F., Bohn, F., Brûna, J., Cailleret, M., François, L., Heinke,
451 J., Henrot, A.J., Hickler, T.: Tree mortality submodels drive simulated long-term forest dynamics:
452 assessing 15 models from the stand to global scale, Ecosphere 10 (2),
453 <https://doi.org/10.1002/ecs2.2616>, 2019
- 454 Cailleret, M., Jansen, S., Robert, E.M., Desoto, L., Aakala, T., Antos, J.A., Beikircher, B.,
455 Bigler, C., Bugmann, H., Caccianiga, M.: A synthesis of radial growth patterns preceding tree
456 mortality, Glob. Chang. Biol. 23, 1675–1690, <https://doi.org/10.1111/gcb.13535>, 2017
- 457 Chiba, S.: Understanding the current situation of the damaged forest of Zao *Abies Mariesii*,
458 efforts for regeneration (In Japanese), 2017
- 459 Chiba, S., Kawatsu, S., Hayashida, M.: Large-area Mapping of the Mass Mortality and
460 Subsequent Regeneration of *Abies Mariesii* Forests in the Zao Mountains in Northern Japan, J Jpn
461 for Soc 102 (1), 108-114, <https://doi.org/10.4005/jjfs.102.108>, 2020



- 462 Cole, W.E., Amman, G.D.: Mountain pine beetle dynamics in lodgepole pine forests, Part
463 1: Course of an infestation, Bark Beetles, Fuels, Fire Bibl., 72, 1980
- 464 Conciatori, M., Tran, N.T.C., Diez, Y., Valletta, A., Segalini, A., Lopez Caceres, M.L.:
465 Plant Species Classification and Biodiversity Estimation from UAV Images with Deep Learning,
466 Remote Sens., 16, 3654, <https://doi.org/10.3390/rs16193654>, 2024
- 467 Cook, E.R., Krusic, P.J.: Program ARSTAN, A tree-ring standardization program based on
468 detrending and autoregressive timeseries modeling with interactive graphics, Tree-Ring
469 Laboratory, Lamont-Doherty Earth Observatory, Columbia University, Palisades, NY, 2005
- 470 Dulamsuren, C., Haucka, M., Leuschnerb, H.H., Leuschnera, C.: Gypsy moth-induced
471 growth decline of *Larix sibirica* in a forest-steppe ecotone, Dendrochronologia, 28 (4): 207-213,
472 <https://doi.org/10.1016/j.dendro.2009.05.007>, 2010
- 473 Farquhar, G.D., O'Leary, M.H.O., Berry, J., A.: On the Relationship between Carbon
474 Isotope Discrimination and the Intercellular Carbon Dioxide Concentration in Leaves, Functional
475 Plant Biology, 9, 121-137, 1982
- 476 Farquhar, G.D., Richards, R., A.: Isotopic Composition of Plant Carbon Correlates with
477 Water-Use Efficiency of Wheat Genotypes, Australian Journal of Plant Physiology, 11(6) 539-
478 552, <https://doi.org/10.1071/PP9840539>, 1984
- 479 Gessler, A., Kreuzwieser, J., Dopatka, T., Rennenberg H.: Diurnal courses of ammonium
480 net uptake by the roots of adult beech (*Fagus sylvatica*) and spruce (*Picea abies*) trees, Plant Soil
481 240:23-32, <https://doi.org/10.1023/A:1015831304911>, 2002
- 482 Grissino-Mayer, H.D.: Evaluating Crossdating Accuracy: A Manual and Tutorial for the
483 Computer Program COFECHA, Tree-Ring Research, 57, 205-221, 2001



- 484 Harsch, M.A., Hulme, P., Mcglone, M., Duncan, R.P.: Are treelines advancing? A global
485 meta-analysis of treeline response to climate warming. *Ecology Letters*, *Ecology Letters*, 12 (10):
486 1040-9, <https://doi.org/10.1111/j.1461-0248.2009.01355.x>, 2009
- 487 Holmes, R.L.: Computer-Assisted Quality Control in Tree-Ring Dating and Measurement,
488 *Environmental Science, Computer Science, Tree-ring Bulletin*, 1983
- 489 Hu, W., Wang, F., Yin, Q., Zhang, F.: SGT: A Generalized Processing Model for 1-D
490 Remote Sensing Signal Classification, *IEEE Geosci. Remote. Sens. Lett.* 19: 1-5,
491 <https://doi.org/10.1109/LGRS.2022.3224933>, 2022
- 492 Jactel, H., Koricheva, J., Castagneyrol, B.: Responses of forest insect pests to climate
493 change: not so simple, *Current opinion in insect science*, 35, 103-108,
494 <https://doi.org/10.1016/j.cois.2019.07.010>, 2019
- 495 Kerchev, I.A.: Ecology of four-eyed fir bark beetle *Polygraphus proximus* Blandford
496 (Coleoptera; Curculionidae, Scolytinae) in the west Siberian region of invasion, *Russian journal*
497 *of biological invasions*, 5(3), 176-185, <https://doi.org/10.1134/S2075111714030072>, 2014
- 498 Kharuk, V.I., Shushpanov, A.S., Petrov, I.A., Demidko, D.A., Im, S.T., Knorre, A.A.: Fir
499 (*Abies sibirica* Ledeb.) mortality in mountain forests of the Eastern Sayan Ridge, Siberia,
500 *Contemp. Probl. Ecol.* 12, 299-309, <https://doi.org/10.1134/S199542551904005X>, 2019
- 501 Koizumi, C.: Beetle infestation associated with the cutting operations in the spruce fir-
502 forest in Hokkaido (in Japanese), *Bull Gov for Exp Stn* 297, 1-34, 1977
- 503 Kolb, T., Keefover-Ring, K., Burr, S.J., Hofstetter, R., Gaylord, M., Raffa, K.F.:
504 Droughtmediated changes in tree physiological processes weaken tree defenses to bark beetle
505 attack, *J. Chem. Ecol.* 45, 888-900, <https://doi.org/10.1007/s10886-019-01105-0>, 2019
- 506 Kononov, A., Ustyantsev, K., Blinov, A., Fet, V., Baranchikov, Y.N.: Genetic diversity of
507 aboriginal and invasive populations of four-eyed fir bark beetle *Polygraphus proximus* Blandford



508 (Coleoptera, Curculionidae, Scolytinae), Agricultural and forest Entomology, 18, 294-301

509 <https://doi.org/10.1111/afe.12161>, 2016

510 Leavitt S. W.: Tree-ring isotopic pooling without regard to mass: No difference from

511 averaging $\delta^{13}\text{C}$ values of each tree, Chemical Geology, 252, 52-55,

512 <https://doi.org/10.1016/j.chemgeo.2008.01.014>, 2008

513 Loader, N. J., Young, G. H. F., Grudd, H., McCarroll, D.: Stable carbon isotopes from

514 Torneträsk, northern Sweden provide amillennial length reconstruction of summer sunshine and

515 its relationship to Arctic circulation, Quaternary Science Reviews, 62, 97-113,

516 <https://doi.org/10.1016/j.quascirev.2012.11.014>, 2013

517 Lopez Caceres, M.L., Nakano, S., Ferrio, J.P., Hayashi, M., Nakatsuka, T., Sano, M.,

518 Yamanaka, T., Nobori, Y.: Evaluation of the effect of the 2011 Tsunami on coastal forests by

519 means of multiple isotopic analyses of tree rings, Isotopes in Environmental and Health Studies

520 54(5):494-507, <https://doi.org/10.1080/10256016.2018.1495203>, 2018

521 Louis, M., Grégoire, J.-C., Péllisson, P.-F.: Exploiting fugitive resources: How long-lived

522 is «fugitive»? Fallen trees are a long-lasting reward for *Ips typographus* (Coleoptera,

523 Curculionidae, Scolytinae), Forest Ecology and Management 331 (6): 129-134,

524 <https://doi.org/10.1016/j.foreco.2014.08.009>, 2014

525 Louis, M., Dohet, L., Gregoire, J.-C.: Fallen trees' last stand against bark beetles, Forest

526 Ecology and Management 359: 44-50, <https://doi.org/10.1016/j.foreco.2015.09.046>, 2016

527 McCarroll, D., Loader, N.J.: Stable isotopes in tree rings, Quaternary Science Reviews 23,

528 771-801, <https://doi.org/10.1016/j.quascirev.2003.06.017>, 2004

529 McCarroll, D., Whitney, M., Young, G.H.F., Loader, N.J., Gagen, M.H.: A simple stable

530 carbon isotope method for investigating changes in the use of recent versus old carbon in oak, Tree

531 Physiol. 37, 1021-1027, <https://doi.org/10.1093/treephys/tpx030>, 2017



- 532 McClung, D.M.: The effects of El Niño and La Niña on snow and avalanche patterns in
533 British Columbia, Canada, and central Chile, *Journal of Glaciology*, 59 (216), 783-792,
534 <https://doi.org/10.3189/2013JoG12J192>, 2013
- 535 Nguyen, H.T., Lopez Caceres, M.L., Moritake, K., Kentsch, S., Shu, H., Diez, Y.:
536 Individual sick fir tree (*Abies mariesii*) identification in insect infested forests by means of UAV
537 images and deep learning, *Remote Sens.* 13, 260, <https://doi.org/10.3390/rs13020260>, 2021
- 538 Nobuchi, A.: Bark-beetles injurious to pine in Japan, Bark-beetles injurious to pine in Japan
539 (in Japanese), *Bull Gov for Exp Sta* 185:1-49, 1966
- 540 Pavlov, I.N., Litovka, Y.A., Golubev, D.V., Astapenko, S.A., Chromogin, P.V., Usoltseva,
541 Y.V., Makolova, P.V. and Petrenko, S.M.: Mass Reproduction of *Polygraphus proximus*
542 Blandford in Fir Forests of Siberia Infected with Root and Stem Pathogens: Monitoring, Patterns,
543 and Biological Control, *Contemporary Problems of Ecology*, 13 (1), pp.71-84,
544 <https://doi.org/10.1134/S1995425520010060>, 2020
- 545 Przepiora, F., Loch, J., Ciach, M., Bark beetle infestation spots as biodiversity hotspots:
546 Canopy gaps resulting from insect outbreaks enhance the species richness, diversity and
547 abundance of birds breeding in coniferous forests, *Forest Ecology and Management* 473, 118,
548 <https://doi.org/10.1016/j.foreco.2020.118280>, 2020
- 549 Rossi, S., Deslauriers, A., Anfodillo, T., Carrer, M.: Age - dependent xylogenesis in
550 timberline conifers, *New Phytologist*, 177 (1), 199-208, [https://doi.org/10.1111/j.1469-](https://doi.org/10.1111/j.1469-8137.2007.02235.x)
551 8137.2007.02235.x, 2008
- 552 Ryan, M. G., Yoder, B. J.: Hydraulic limits to tree height and tree growth, *Bioscience* 47,
553 235-242, <https://doi.org/10.2307/1313077>, 1997
- 554 Schindler, D., Bauhus, J., Mayer, H.: Wind effects on trees, *European Journal of Forest*
555 Research, 131: 159-163, <https://doi.org/10.1007/s10342-011-0582-5>, 2011



- 556 Schweingruber, F. H.: Tree rings - basics and applications of dendrochronology, Kluwer
557 Academic Publishers, ISBN 90277244 58, 276 p., 1988
- 558 Stokes, M.A., Smiley, T.L.: An Introduction to Tree-ring Dating, University of Arizona
559 Press, 73 p., 1996
- 560 Takagi, E., Masaki, D., Kanai, R., Sato, M., Iguchi, K.: Mass mortality of *Abies veitchii*
561 caused by *Polygraphus proximus* associated with tree trunk diameter in Japan, Forest Ecology and
562 Management, 428, 14-19, <https://doi.org/10.1016/j.foreco.2018.06.030>, 2018
- 563 Takagi, E., Masaki, D., Kōbayashi, K., Takei, S.: Trunk diameter influences attack by
564 *Polygraphus proximus* and subsequent mortality of *Abies veitchii*, Forest Ecology and
565 Management, 479, <https://doi.org/10.1016/j.foreco.2020.118617>, 2021
- 566 Tanaka, N., Matsui, T.: PRDB: Phytosociological Releve Database, Forestry and Forest
567 Products Research Institute, <http://www.ffpri.affrc.go.jp/labs/prdb/index.html>, 2007
- 568 Timofeeva, G., Treydte, K., Bugmann, H., Rigling, A., Schaub, M., Siegwolf, R., Saurer,
569 M.: Long - term effects of drought on tree - ring growth and carbon isotope variability in Scots
570 pine in a dry environment, Tree Physiology, 37 (8), 1028-1041,
571 <https://doi.org/10.1093/treephys/tpx041>, 2017
- 572 Tokuda, M., Shoubu, M., Yamaguchi, D., Yukawa, J.: Defoliation and dieback of *Abies*
573 *firma* (Pinaceae) trees caused by *Parendaeus abietinus* (Coleoptera: Curculionidae) and
574 *Polygraphus proximus* (Coleoptera: Scolytidae) on Mount Unzen, Japan, Applied entomology and
575 zoology, 43 (1), 1-10, <https://doi.org/10.1303/aez.2008.1>, 2008
- 576 Tran, T.C.N., Lopez Caceres, M.L., Riera, S.G.i., Conciatori, M., Kuwabara, Y., Tsou, C.-
577 Y., Diez, Y.: Using UAV RGB Images for Assessing Tree Species Diversity in Elevation Gradient
578 of Zao Mountains, s. Remote Sens. 2024, 16, 3831, <https://doi.org/10.3390/rs16203831>, 2024



579 Ulrich, W., Kusumoto, B., Shiono, T., Fuji, A., Kubota, Y.: Latitudinal gradients of
580 reproductive traits in Japanese woody plants, *Ecological Research* 38 (1),
581 <https://doi.org/10.1111/1440-1703.12363>, 2022

582 Van Lierop, P., Lindquist, E., Sathyapala, S. and Franceschini, G.: Global Forest area
583 disturbance from fire, insect pests, diseases and severe weather events, *Forest Ecology and*
584 *Management*, 352, 78-88, <https://doi.org/10.1016/j.foreco.2015.06.010>, 2015